Published by Avanti Publishers

Journal of Advanced Thermal Science Research

ISSN (online): 2409-5826

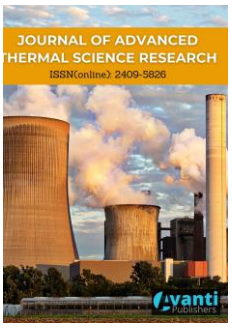

Preparation and Characterization of GG-$LiCF_3SO_3$-DMSO Gel Polymer Electrolyte for Potential Lithium-Ion Battery Application

N.M.A.C. Daud[1], N. Tamchek[1] and I.M. Noor[1,2,*]

[1]*Ionic Materials and Energy Devices Laboratory, Department of Physics, Faculty of Science, Universiti Putra Malaysia, 43400 UPM Serdang, Selangor Darul Ehsan, Malaysia*

[2]*Physics Division, Centre of Foundation Studies for Agricultural Science, Universiti Putra Malaysia, 43400 UPM Serdang, Selangor Darul Ehsan, Malaysia*

ARTICLE INFO

Article Type: Research Article

Keywords:
Lithium-ion battery
Charge carrier mobility
Equivalent circuit model
Charge carrier concentration
Conductivity-temperature dependent

Timeline:
Received: July 18, 2022
Accepted: September 21, 2022
Published: October 20, 2022

Citation: Daud NMAC, Tamchek N, Noor IM. Preparation and characterization of GG-$LiCF_3SO_3$-DMSO gel polymer electrolyte for potential lithium-ion battery application. J Adv Therm Sci Res. 2022; 9: 69-83.

DOI: https://doi.org/10.15377/2409-5826.2022.09.6

ABSTRACT

This work uses gellan gum (GG) natural polymer as the base polymer to prepare gel polymer electrolytes (GPEs). Lithium trifluoromethanesulfonate ($LiCF_3SO_3$) salt is used as a charge supplier, and dimethyl sulfoxide (DMSO) acts as a plasticizer to keep the electrolyte in gel form. Two electrolyte systems are formed, which are $LiCF_3SO_3$-DMSO liquid electrolytes and GG-$LiCF_3SO_3$-DMSO GPEs. Liquid electrolyte with a composition of 12.42 wt.% $LiCF_3SO_3$-87.58 wt.% DMSO (LN3 electrolyte) revealed the highest room temperature conductivity (σ_{rt}) of 9.14 mS cm^{-1}. The highest σ_{rt} value obtained by the LN3 electrolyte is strongly influenced by the charge carrier concentration (n) relative to the mobility (μ). To form GPEs, GG is added to the LN3 electrolyte since this sample composition gave the highest σ_{rt}. The electrolyte of 2.00 wt.% GG-12.18 wt.% $LiCF_3SO_3$-85.82 wt.% DMSO (GN3 electrolyte) showed the highest σ_{rt} of 9.96 mS cm^{-1}. The highest σ_{rt} value obtained by GN3 electrolyte is strongly influenced by μ rather than n. The conductivity-temperature study showed that the increase in conductivity for GG-$LiCF_3SO_3$-DMSO GPEs is controlled by an increase in n, not μ. Linear sweep voltammetry (LSV) for the GN3 electrolyte showed high electrochemical stability up to 4.8 V. Cyclic voltammetry (CV) illustrated the redox process in the GN3 electrolyte is reversible. A lithium-ion battery fabricated with GN3 electrolyte showed a good discharge performance up to 480 hours with an average voltage of 1.50 V discharged at a current of 0.001 mA. Based on this work, it can be concluded that natural polymer GG-based GPE has great potential for use in LIBs as a charge transport medium.

*Corresponding Author
Email: imnoor@upm.edu.my
Tel: +(60) 39769 3138

1. Introduction

Over the past ten years, the demand for the lithium-ion technology in electric vehicles and portable devices has increased rapidly. According to a report from Bloomberg [1], the demand for lithium-ion technology is 526 GWh in 2020, which is expected to increase further to approximately 9300 GWh by 2030. This is due to the proliferation of new electric vehicles, storage containers, and portable devices such as smartphones, laptops, etc. Lithium-ion batteries (LIBs) have been widely used in grid energy storage, electronic devices, electric vehicles, etc., over the past decades due to their high specific energy density and stable cycling performance [2]. In LIBs, electrolyte plays an important role as a medium for ion conduction. Free ions will flow and accumulate on the corresponding electrode to act as energy storage devices when an electric field is applied across the cell. Most LIBs used liquid electrolytes [3, 4]. Because liquid electrolytes are easy to leak, research has focused on using polymer electrolytes as separators in LIBs [5, 6].

The use of polymer electrolytes has grown dramatically due to the positive impact of LIB applications. Polymer electrolytes are reported to provide good electrode-electrolyte contact [7], high energy density [8], and high ionic conductivity [9] in LIBs. As a result, a lot of vigorous research is being conducted on polymer electrolyte materials. Polymer electrolytes are generally used as synthetic polymers, such as polyethylene oxide (PEO) [10,11], polyvinyl chloride (PVC) [12], polymethyl methacrylate (PMMA) [13], and polystyrene (PS) [14] as base materials. However, the synthetic polymers commonly used have a few downsides: poor biocompatibility, non-degradable, expensive, and not ecological-friendly [15]. Along with the world of eco-technology and environmental sustainability, research on using natural polymers to replace standard synthetic polymers is actively underway.

Natural polymer is a naturally created material based on living organisms [16]. Chitosan [17], gelatin [18], cellulose [19], starch [20], pectin [21], alginate [22], carrageenan [23], and gellan gum [24] are examples of natural polymers. It was found that natural polymers have excess electrons in their chemical structure. This property allows natural polymers to coordinate with free ions dissociated from the complex salts, making them suitable for use as host polymers in electrolytes. Besides, natural polymers are non-toxic, biodegradable, sustainable, have good chemical and physical properties, are low-cost, and are generally available [15], which provides benefits to replacing synthetic polymers, especially in energy storage systems. These natural polymers can be important solutions to various ecological problems such as pollution and resources sustainability if duly employed.

Gellan gum (GG) is a water-soluble anionic polysaccharide produced through the fermentation process of *the Pseudomonas elodea* microorganism [25]. Polysaccharides are known to be naturally abundant, cheap, and environmentally friendly [26]. GG is an exopolysaccharide in which the chemical structure of GG consists of a backbone with a repeating unit of β–D–glucose (D–Glc), L–rhamnose (L–Rha), and D–glucuronic acid (D–GlcA) as well as two acyl groups namely acetate and glycerate, bound to the glucose residues adjacent to glucuronic acid [27]. GG is safe for human consumption, so it has been widely used as a stabilizer and thickener in food and processing industries that require gelling, texturizing, suspending, and film-forming [28]. GG is reported to have high thermal stability up to 507 K and high thermal reversibility properties [25,29]. Figure **1** shows the chemical structure of GG. It can be seen that GG contains two hydroxymethyl groups and one carboxyl group per repeating unit with hydroxyl (OH), ether (C-O-C), and carboxyl (COOH) groups on its polymer matrix. These functional groups have an excess of electrons on the oxygen atom that allows the free cations dissociated from complex salt to coordinate, thus making it the right choice for polymer host in electrolytes. Halim *et al.* [29] reported that a solid polymer electrolyte (SPE) consists of 54 wt.% gellan gum, 36 wt.% LiI and 10 wt.% glycerol have revealed a maximum conductivity of 1.5×10^{-3} S cm^{-1} at room temperature. Noor *et al.* [24] also recorded a GG-based SPE complex with 40 wt.% $LiCF_3SO_3$ has shown a maximum room temperature ionic conductivity of 5.38×10^{-4} S cm^{-1}. Neto *et al.* [30] exposed the use of GG:IL: $LiCF_3SO_3$ in a ratio of 5:1:10 with a conductivity of 6.46×10^{-3} S cm^{-1} in electrochromic devices has improved the performance of the devices. These findings suggest that GG has a high potential to be a polymer host and ion conduction separator medium in LIBs.

Based on our literature investigation, several types of natural polymers are used as hosts in polymer electrolytes and applied in LIBs. Therefore, this work is undertaken to produce a new polymer-based electrolyte for potential applications in LIBs. In this work, GG-based gel polymer electrolytes (GPEs) were prepared. The GPEs

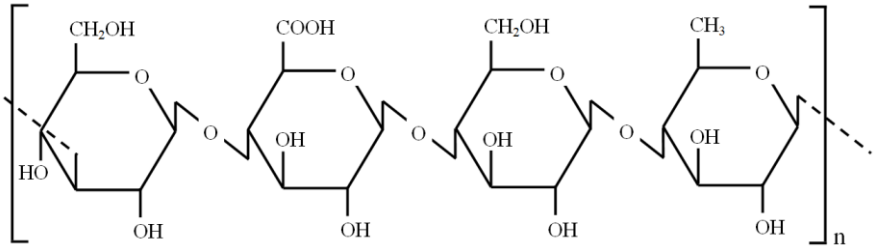

Figure 1: Chemical structure of gellan gum.

have the advantage of high ionic conductivity as liquid electrolytes compared to other types of polymer electrolytes and non-leak [31]. GPEs are formed by trapping a liquid electrolyte between the polymer matrix to make it semi-solid colloidal. To investigate the impact of GG in the electrolyte system, different amounts of GG were added to the highest conducting liquid electrolyte consisting of lithium trifluoromethanesulfonate ($LiCF_3SO_3$) in dimethyl sulfoxide (DMSO). The electrical properties of GG-$LiCF_3SO_3$-DMSO GPEs at room and elevated temperatures were evaluated. The highest conducting sample was then used to study its electrochemical properties using linear sweep voltammetry and cyclic voltammetry. The potential for the highest conductivity of GG-$LiCF_3SO_3$-DMSO GPE in lithium-ion batteries was then tested by performing battery-discharge measurements.

2. Experimental

2.1. Materials

Gellan gum (GG) was purchased from Duchefa Company, Netherland (Gelrite Cat. No: G1101). Dimethyl sulfoxide (DMSO; anhydrous ≥99.9%) and lithium trifluoromethanesulfonate ($LiCF_3SO_3$; 96% assay) were procured from Sigma Aldrich. Before use, GG and $LiCF_3SO_3$ were dried in a vacuum oven for 24 h at 323 K. Other materials were used as received.

2.2. Preparation of $LiCF_3SO_3$-DMSO Liquid Electrolytes

$LiCF_3SO_3$-DMSO liquid electrolytes (LEs) were prepared in the first stage of sample preparation. The desired amount of $LiCF_3SO_3$, as shown in Table **1**, was mixed with 3.0 g of DMSO in a closed bottle. The mixture was then stirred for 1 h at a temperature of 343 K with low rotational speed using a magnetic stirrer until a homogenous solution of $LiCF_3SO_3$-DMSO was formed. Then, the mixture was left to cool to room temperature. The prepared LEs were stored in a desiccator overnight before being used for characterization.

Table 1: Designation and sample composition for $LiCF_3SO_3$-DMSO liquid electrolyte system.

Designation	$LiCF_3SO_3$ (Molarity)	DMSO (g)	$LiCF_3SO_3$ (g)
LN1	0.60	3.0	0.2553
LN2	0.80	3.0	0.3404
LN3	1.00	3.0	0.4255
LN4	1.20	3.0	0.5106
LN5	1.40	3.0	0.5957

2.3. Preparation of GG-$LiCF_3SO_3$-DMSO Gel Polymer Electrolytes

The LE composition of $LiCF_3SO_3$-DMSO with the highest room temperature conductivity obtained from electrical impedance spectroscopy (EIS) was selected as a reference for the preparation of the GPE system. The 12.42 wt.% $LiCF_3SO_3$-87.58 wt.% DMSO electrolyte (LN3 electrolyte) was chosen due to its highest room

temperature conductivity of 9.14 mS cm^{-1} obtained from EIS. As listed in Table **2**, the corresponding amount of GG was added to 3.4255 g of LN3 electrolyte. The mixture was stirred for 4 h at a temperature of 343 K with low rotational speed using a magnetic stirrer. The homogenous GG-$LiCF_3SO_3$-DMSO GPEs were then left to cool to room temperature and stored in a desiccator overnight before being used for characterization.

Table 2: Designation and sample composition for GG-$LiCF_3SO_3$-DMSO GPE system.

Designation	GG : $LiCF_3SO_3$: DMSO (wt.% : wt.% : wt.%)	GG (g)	$LiCF_3SO_3$ (g)	DMSO (g)
GN1	1.44: 12.24: 86.32	0.0500	0.4255	3.0
GN2	1.72: 12.21: 86.07	0.0600	0.4255	3.0
GN3	2.00: 12.18: 85.82	0.0700	0.4255	3.0
GN4	2.28: 12.14: 85.58	0.0800	0.4255	3.0

2.4. Electrolyte Characterizations

2.4.1. Electrical Impedance Spectroscopy (EIS)

EIS was carried out to estimate the ionic transport properties of the prepared LEs and GPEs. The LEs and GPEs are each filled in a coin cell with stainless steel plates and clamped in a cell holder. The cell holder was then connected to a cable connected directly to the LCR meter HIOKI 3520 LCR Hi-Tester. A small sinusoidal *ac* voltage of 10 mV with a frequency range between 50 Hz and 100 kHz was then applied across the sample. The measurements were conducted from 300 K (room temperature) to 373 K. From the data obtained, the bulk resistance (*R*) can be determined from the plot of negative imaginary impedance (−*Z*″) against actual impedance (*Z*′), which is known as Nyquist plot. The bulk resistance value was then substituted in equation (1) to estimate the ionic conductivity (σ) value of the sample:

$$\sigma = \frac{t}{A \times R} \tag{1}$$

In equation (1), *t* represents the sample thickness (0.26 cm), while *A* refers to the electrode-electrolyte contact area (2.011 cm^2).

2.4.2. Linear Sweep Voltammetry (LSV)

The LSV is an electrochemical technique used to determine the cut-off voltage of an electrolyte. In this work, 2.00 wt.% GG-12.18 wt.% $LiCF_3SO_3$-85.82 wt.% DMSO GPE (GN3 electrolyte) was used to test their electrochemical performance as this electrolyte composition revealed the highest conductivity at room temperature, which was then used in the battery-discharge measurement. The GN3 electrolyte was sandwiched between stainless steel acting as a working electrode and lithium metal as counter and reference electrode and clamped together in a coin cell. The coin cell was then placed in a cell holder and wrapped with parafilm. All preparations were carried out in an argon-filled glove box to avoid moisture that could destroy the lithium metal and break down the cell. The cell holder was then connected to a cable connected directly to the CH Instruments model 660C. A voltage from 0 V (lower limit) to 8.0 V (upper limit) was applied across the sample, and the current through the sample was measured. The cut-off voltage for the GN3 electrolyte was then determined from the intercept of the slope with the horizontal axis through the current versus voltage voltammogram.

2.4.3. Cyclic Voltammetry (CV)

The CV was carried out to obtain information about the electrochemical stability of the sample. The GN3 electrolyte was sandwiched between stainless steel acting as the working electrode and lithium metal as the counter and reference electrode and clamped together in a coin cell. The coin cell was then placed in a cell holder and wrapped with parafilm. All preparations were carried out in an argon-filled glove box to avoid moisture that

could destroy the lithium metal and break down the cell. The cell holder was then connected to a cable connected directly to the CH Instruments model 660C. Cyclic voltammetry was performed by applying an alternating potential between specific upper and lower limits. The current flowing in the electrolyte was recorded. CV measurement was performed for 9 cycles to investigate the cycle stability of the electrolyte.

2.5. Fabrication and Characterization of Lithium-Ion Battery (LIB)

The LIB was fabricated to test the potential of the highest conducting GPE in storage energy devices. GPE with 2.00 wt.% GG-12.18 wt.% $LiCF_3SO_3$-85.82 wt.% DMSO (GN3 electrolyte) was placed between graphite that acts as the cathode and the lithium metal acting as the anode in the configuration of graphite/GN3/Li metal. All materials were clamped in a CR2032 coin cell. The coin cell was then placed in a stainless-steel cell holder and wrapped with parafilm. All assembly processes were performed in an argon-filled glove box to avoid moisture that could destroy the lithium metal and break down the cell. The cell was then subjected to a 0.001 mA discharge current at room temperature using the Netware battery cycler.

3. Results and Discussion

3.1. Ionic Transport Properties of $LiCF_3SO_3$-DMSO Liquid Electrolytes

Figure **2** shows the Nyquist plot for $LiCF_3SO_3$-DMSO LEs at room temperature (300 K). The plot shows only a titled spike shape, indicating materials' high conducting nature. The bulk resistance (*R*) value is obtained from the intersection of the plot with the horizontal axis. The conductivity of $LiCF_3SO_3$-DMSO LEs is calculated from equation (1) using the *R*-value obtained in Figure **2**. The variation of room temperature conductivity for DMSO with different $LiCF_3SO_3$ salt concentrations is depicted in Figure **3(a)**.

From Figure **3(a)**, the LN1 electrolyte consists of 0.6 M $LiCF_3SO_3$ giving a conductivity value of 6.40 mS cm^{-1}. The conductivity increases gradually until it reaches an optimum value of 9.14 mS cm^{-1} with an electrolyte of 1.0 M $LiCF_3SO_3$ (LN3 electrolyte). The conductivity decreases to 8.92 mS cm^{-1} and 6.90 mS cm^{-1} after 1.2 M, and 1.4 M of $LiCF_3SO_3$ salts are added to DMSO, respectively.

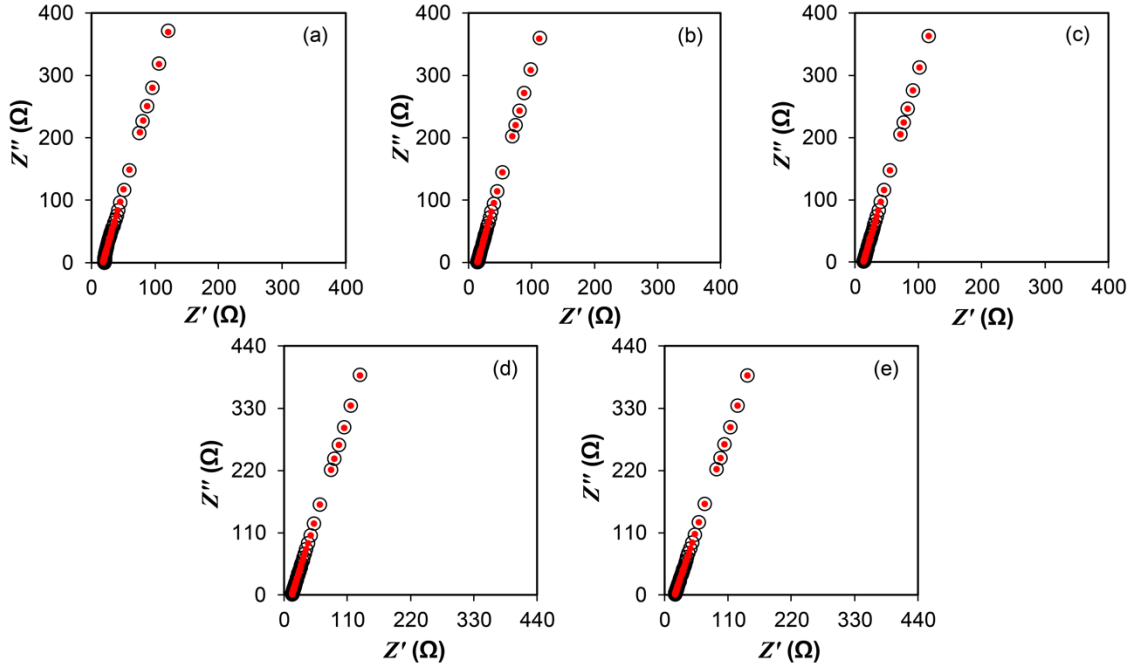

Figure 2: Nyquist plot with the corresponding fitted point for (a) LN1, (b) LN2, (c) LN3, (d) LN4, (e) LN5 at room temperature (o refer to experimental data and ● refer to fitting data).

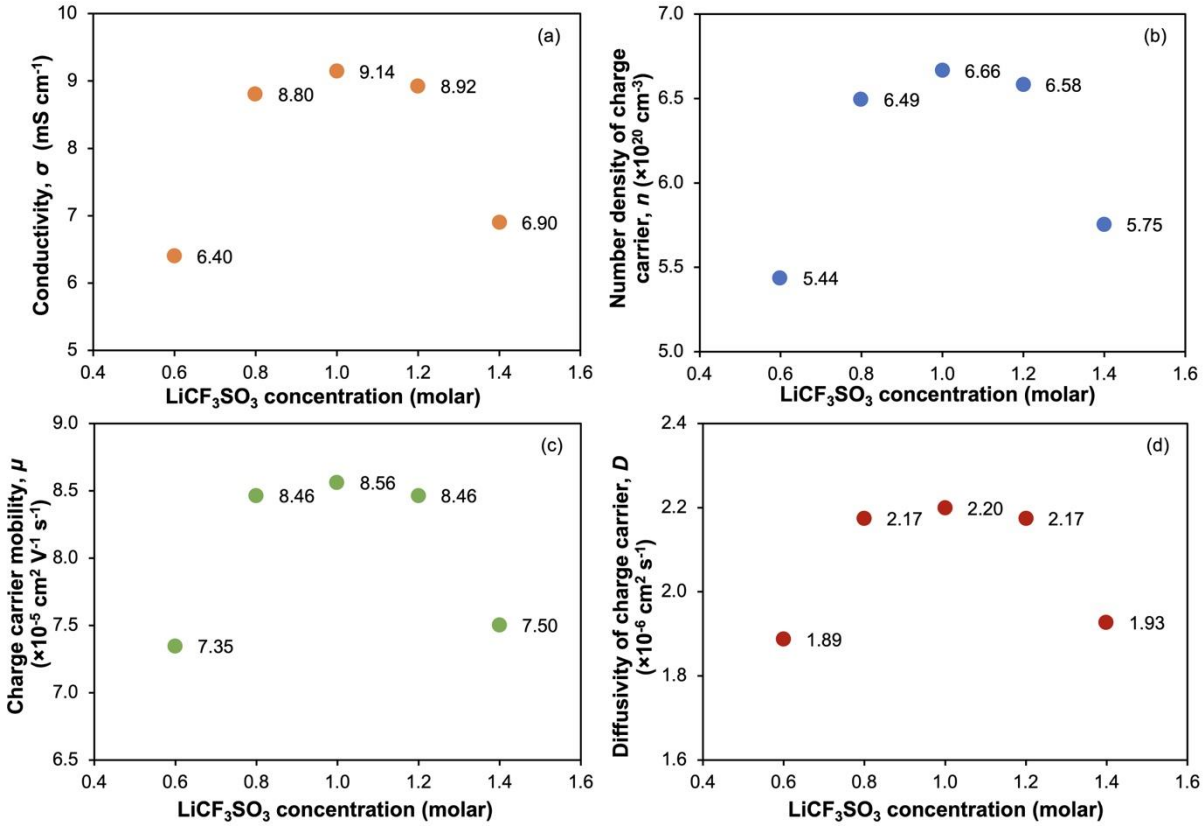

Figure 3: Variation of (a) conductivity, (b) number density, (c) mobility, and (d) diffusivity of charge carrier for $LiCF_3SO_3$-DMSO liquid electrolytes at room temperature.

The conductivity of an electrolyte is strongly related to mobility (μ), diffusivity (D), and number density (n) of the charge carrier. This transport property of the charge carrier is associated with the conductivity (σ) according to equation (2) [32].

$$\sigma = n\mu e \tag{2}$$

Here, n is the charge carrier's number density, μ is the charge carrier's mobility, and e is the electron's charge. From the impedance data, the value of n *and* μ can be estimated by fitting the experimental Nyquist plots with the impendence equation derived from an equivalent circuit that contains a resistor connected in series with a constant phase element (CPE) (Figure **4**) [33]. Based on the equivalent circuit model shown in Figure **4**, the derivative equations for real (Z') and imaginary (Z'') impendence are as below:

$$Z' = R + \frac{\cos\left(\frac{\pi p}{2}\right)}{C\omega^p} \tag{3}$$

$$Z'' = \frac{\sin\left(\frac{\pi p}{2}\right)}{C\omega^p} \tag{4}$$

In equations (3) and (4), R is the electrolyte bulk resistance, p refers to the gradient parameter that controls the skewness of the titled spike, and ω is the angular frequency. The parameter C is the capacitance at the electrode/electrolyte interface determined by trial and error until the fitted points at the corresponding frequency are matched to the experimental Nyquist plot. All parameter values obtained in the fitting method are then substituted in equations (5), (6), and (7) to estimate the D, μ and n of the charge carrier in the electrolyte [34,35].

$$D = D_0 \exp\{-0.158[\log_{10}(D_0)]^2 - 3.304[\log_{10}(D_0)] - 14.504\} \quad (5)$$

$$\mu = \frac{eD_0 \exp\{-0.158[\log_{10}(D_0)]^2 - 3.304\left[\log_{10}(D_0)\right] - 14.504\}}{k_b T} \quad (6)$$

$$n = \frac{\sigma k_b T}{e^2 D_0 \exp\{-0.158[\log_{10}(D_0)]^2 - 3.304\left[\log_{10}(D_0)\right] - 14.504\}} \quad (7)$$

Here

$$D_0 = \frac{4d^2}{C^4 R^4 \omega_{\min}{}^3} \quad (8)$$

In equations (7) and (8), k_b is the Boltzmann's constant, T is the absolute temperature, σ is the ionic conductivity (obtained from equation (1)), d is the sample thickness, and R is the bulk resistance $\omega_{\min}$. The angular frequency corresponds to the minimum imaginary impedance (at $Z'' \approx 0$). Figures **3(b)**, **3(c)**, and **3(d)** show respectively the charge carrier concentration, mobility, and diffusivity as a function of LiCF$_3$SO$_3$ salt concentration.

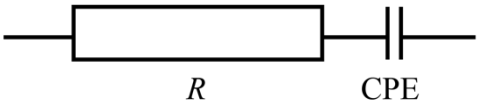

Figure 4: Equivalent circuit that contains a resistor connected in series with a constant phase element (CPE).

Figure **3(b)** shows that the DMSO containing 0.6 M LiCF$_3$SO$_3$ (LN1 electrolyte) has a free ion concentration of 5.44×10^{20} cm^{-3}. These free ions are obtained from salt dissociation with the help of DMSO. DMSO has a dielectric constant of 46.71 [36]. The high dielectric constant of DMSO can break the lattice energy of LiCF$_3$SO$_3$ and dissociate the salt into Li^+ cations and $CF_3SO_3^-$ anions. The number of free ions increases as the amount of LiCF$_3$SO$_3$ salt in the DMSO increases due to the dissociation of more salts which can be observed in Figure **3(b)**. From Figure **3(b)**, the n increases from 5.44×10^{20} cm^{-3} (consisting of 0.6 M LiCF$_3$SO$_3$) to a maximum of 6.66×10^{20} cm^{-3} (consisting of 1.0 M LiCF$_3$SO$_3$). The n decreases as the amount of LiCF$_3$SO$_3$ in DMSO exceeds 1.0 M. The n is seen to further decrease to 5.75×10^{20} cm^{-3} when 1.4 M LiCF$_3$SO$_3$ is added to the DMSO (LN5 electrolyte). The decrease in n can be referred to as the increase of ion association in the electrolyte. More free ions are dissociated when a large amount of salt is added to the polar solvent. Due to the limited space between the ions in the solvent, the free ions tend to remain close to each other, leading to ion association formation. This phenomenon occurs due to the attractive Coulomb force possessed by two opposite charges closer to each other, which induces them to combine [37].

Figure **3(c)** shows the variation of room temperature charge carrier mobility (μ) of LiCF$_3$SO$_3$-DMSO liquid electrolytes. It can be seen that the μ increases from 7.35×10^{-5} cm^2 V^{-1} s^{-1} (LN1 electrolyte) to a maximum of 8.56×10^{-5} cm^2 V^{-1} s^{-1} (LN3 electrolyte) when the amount of LiCF$_3$SO$_3$ in DMSO increases from 0.6 M to 1.0 M. The addition of LiCF$_3$SO$_3$ salt of more than 1.0 M is seen to decrease the μ gradually. This condition occurs due to the increase/decrease of ion collisions between free/pair ions when an electric field is applied across the electrolyte. Figure **3(b)** shows that n is highest in LN3 electrolytes. The n decreases when LiCF$_3$SO$_3$ salt in DMSO exceeds 1.0 M. The decrease in n can be attributed to the increase in ion association. Ion association may influence the flow of free ions in the electrolyte under an applied electric field [37]. This situation causes the ions to slower their motion resulting in lower ionic mobility, as shown in Figure **3(c)**.

From Figure **3(d)**, it can be seen that the D trend is the same as that of μ shown in Figure **3(c)**. According to the Nernst-Einstein equation, the diffusion coefficient of charge is directly proportional to the mobility of charge. Therefore, the trend of μ and D obtained in Figures **3(c)** and **3(d)** are the same. Based on observation from Figures **3(b)**, **3(c)**, and **3(d)**, it can be concluded that the variation of room temperature conductivity in LiCF$_3$SO$_3$-DMSO liquid electrolyte is governed by both the number density and mobility of charge carriers.

To further investigate which parameters most influence the conductivity trend in the $LiCF_3SO_3$-DMSO liquid electrolyte system, a plot of the n to μ ratio as a function of $LiCF_3SO_3$ salt concentration is constructed. Figure **5** shows the n to μ ratio variation for the $LiCF_3SO_3$-DMSO liquid electrolyte system. It can be seen that the LN3 electrolyte reveals the highest ratio of 7.78×10^{24} Vs cm^{-5}. The plot trend in Figure **5** follows the same as the room temperature conductivity shown in Figure **3(a)**. This result implies that the number density of charge carriers predominantly affects the conductivity of $LiCF_3SO_3$-DMSO liquid electrolytes compared to the mobility of charge carriers. It can be concluded that the number density of charge carriers is the dominant factor in controlling the conductivity of $LiCF_3SO_3$-DMSO liquid electrolytes in Figure **3(a)** rather than the mobility and diffusivity of charge carriers.

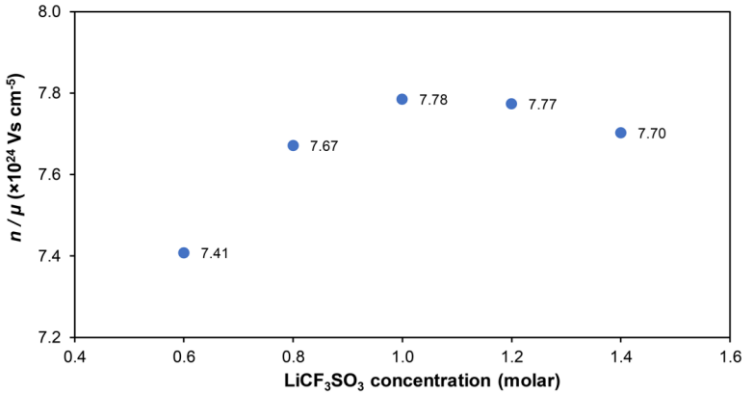

Figure 5: Ratio of n to μ for $LiCF_3SO_3$-DMSO liquid electrolyte system at room temperature.

3.2. Ionic Transport Properties of GG-$LiCF_3SO_3$-DMSO Gel Polymer Electrolytes at Room Temperature

From Figure **3(a)**, the LN3 electrolyte shows the highest room temperature conductivity of 9.14 mS cm^{-1}. The LN3 electrolyte composition was used to form a gel polymer electrolyte by adding different amounts of GG, as tabulated in Table **2**. Electrical impedance spectroscopy is a non-destructive method used in this work to determine the conductivity of GG-$LiCF_3SO_3$-DMSO GPEs. The dynamic ion properties can be evaluated from the data obtained. Figure **6** shows the Nyquist plot for GG-$LiCF_3SO_3$-DMSO GPEs at room temperature. The plot shows only a titled spike shape, indicating materials' high conducting nature. The bulk resistance (R) value is obtained from the intersection of the plot with the horizontal axis. The conductivity of GG-$LiCF_3SO_3$-DMSO GPEs is calculated from equation (1) using the R values obtained in Figure **6**. The variation of room temperature conductivity for GG-$LiCF_3SO_3$-DMSO GPEs is depicted in Figure **7(a)**.

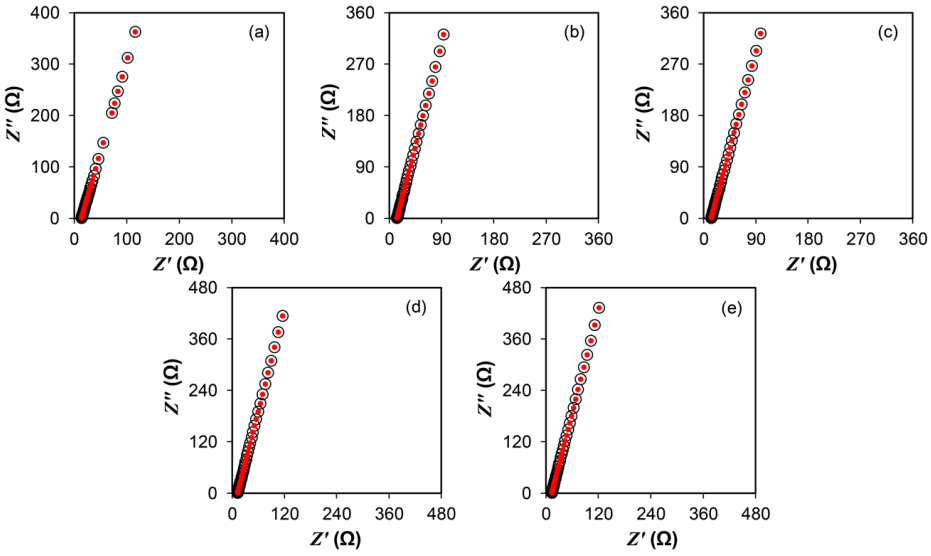

Figure 6: Nyquist plot for (a) LN1, (b) GN1, (c) GN2, (d) GN3, and (e) GN4 electrolyte at room temperature (o refer to experimental data and • refer to fitting data).

From Figure **7(a)**, the GG-free GPE (LN3 electrolyte) has a room temperature ionic conductivity of 9.14 mS cm^{-1}. The addition of GG up to 2.00 wt.% (GN3 electrolyte) gradually increases the electrolyte conductivity up to 9.96 mS cm^{-1}, the maximum conductivity obtained at room temperature for this GPE system. The conductivity of the electrolyte is seen to decrease to 9.41 mS cm^{-1} after 0.28 wt.% GG was added to LN3 electrolyte. The conductivity of an electrolyte is strongly related to the mobility (μ), diffusivity (D), and number density (n) of the charge carrier. Thus, the transport properties of the charge carrier for GG-LiCF$_3$SO$_3$-DMSO GPEs are quantitatively evaluated.

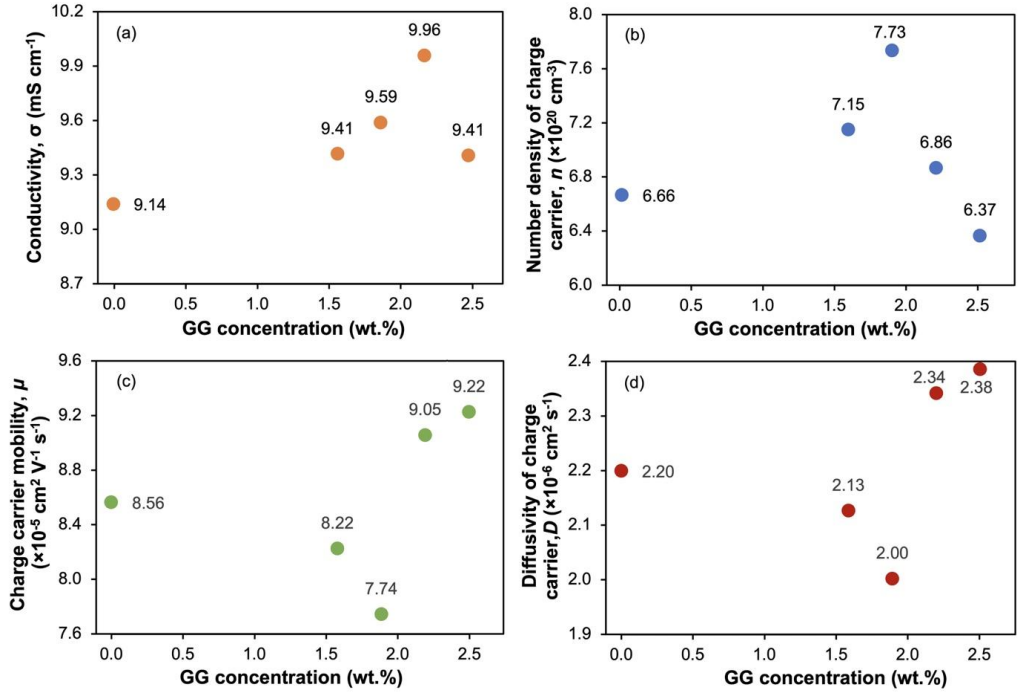

Figure 7: Variation of (a) conductivity, (b) number density, (c) mobility, and (d) diffusivity of charge carrier for GG-LiCF$_3$SO$_3$-DMSO GPE system at room temperature.

3.3. Evaluation of Ionic Transport Properties at Room Temperature

Figure **7(b)** shows the variation of charge carrier density (n) for the GG-LiCF$_3$SO$_3$-DMSO GPE system at room temperature. It can be seen that n in LN3 electrolyte (GG-free electrolyte) is 6.66×10^{20} cm^{-3}. It shows an increasing trend when the amount of GG increases up to 1.72 wt.% with 7.73×10^{20} cm^{-3} free ion concentration. As mentioned earlier, the LiCF$_3$SO$_3$ is attracted by an ionic bond. Adding GG into the LiCF$_3$SO$_3$-DMSO liquid electrolyte (LN3 electrolyte) leads to the dissociation of more free ions. This is because GG natural polymer has excess electrons on its structural heteroatom that aid the LiCF$_3$SO$_3$ salt to dissociate and form coordination with its polymer matrix, resulting in an increase in the number of free ions in the electrolyte. The n is observed to decrease gradually when the amount of GG in the LN3 electrolyte is more than 1.72 wt.%. The decrease in n is due to less space and distance for Li^+ and $CF_3SO_3^-$ to move around as the GG concentration has increased, resulting in the formation of association ions. The free ions get close and attract each other by Coulomb force [38]. A pair of neutral ion charges is formed when ions are attracted to each other. This ion is known as ion association. Therefore, the number of free ions in the GPE decreases and causes a reduction in the number density of charge carriers, as observed in Figure **7(b)**.

From Figure **7(b)**, the n shows an increasing trend until it reaches an optimal value of 7.73×10^{20} cm^{-3} for GPE with 1.72 wt.% GG. The μ and D of charge carriers in Figures **7(c)** and **7(d)** show the opposite trend to n. The μ is observed to decrease from 8.56×10^{-5} cm^2 V^{-1}s^{-1} (LN3 electrolyte) to 7.74×10^{-5} cm^2 V^{-1}s^{-1} (GN2 electrolyte). The D decreases from 2.20×10^{-6} cm^2 s^{-1} to 2.00×10^{-6} cm^2 s^{-1}. The decrease in μ and D can be attributed to the increase in ion collisions between free ions due to the increase in n. Ion collisions cause the movement of free ions to slow down, thus reducing μ and D, as obtained in Figures **7(c)** and **7(d)**, respectively. When the amount of GG in LN3 electrolyte is more than 1.72 wt.%, n decreases (see Figure **7(b)**). The μ and D are observed to increase (see Figures

7(c) and **7(d)**). This phenomenon occurs due to the formation of ion association that reduces the *n*. The remaining free ions move randomly in the electrolyte medium. Although free ions have less space to move under an applied electrical field, the free ions can travel easily and have less collisions between them. This enhances ion drift which in turn increases the mobility as well as the diffusion coefficient of the free ion [38].

To investigate which parameters most influence the conductivity trend in the GG-$LiCF_3SO_3$-DMSO GPE system, a plot of *n* to μ ratio as a function of GG concentration is constructed. Figure **8** shows the *n* to μ ratio variation for the GG-$LiCF_3SO_3$-DMSO GPE system. It can be seen that the GN2 electrolyte shows the highest ratio of 9.99×10^{24} Vs. cm^{-5}. The trend of the plot for LN3, GN1, and GN2 electrolytes in Figure **8** is observed to follow the same trend as the room temperature conductivity shown in Figure **7(a)**. This implies that the charge carrier density is primely influencing the conductivity of LN3, GN1, and GN2 electrolytes compared to the charge carrier mobility. GN3 electrolyte shows the highest room temperature conductivity. The highest conductivity obtained in GN3 electrolyte is dominantly influenced by the mobility of the charge carrier than the charge carrier density, as observed in Figure **8**. It can be concluded that the concentration and mobility of charge carriers play an important role in controlling the conductivity of the GG-$LiCF_3SO_3$-DMSO GPE system.

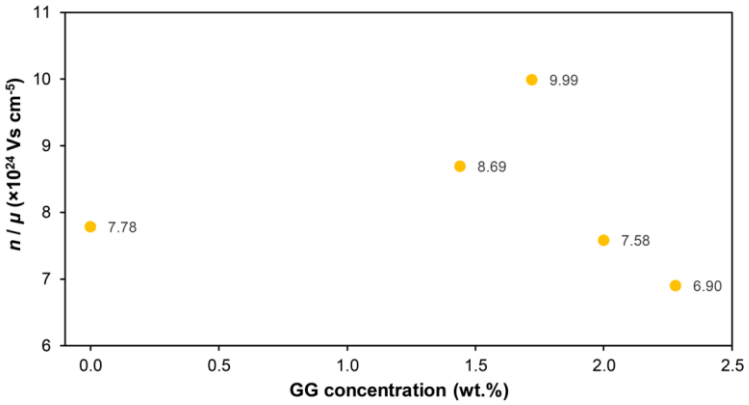

Figure 8: Ratio of *n* to μ in GG-$LiCF_3SO_3$-DMSO GPE system at room temperature.

3.4. Conductivity-Temperature Dependence

Figure **9** shows the conductivity plot as a temperature function for GG-$LiCF_3SO_3$-DMSO GPEs. It can be seen that the conductivity for all GPEs increased with increasing temperature, from 300 K to 373 K. As observed in Figure **9**, the plots for all samples mostly overlapped at several temperatures. It is because the conductivity value for each sample at most temperatures is close. To further understand the factor that influenced the conductivity-temperature trend, the impedance data for all GPEs at various temperatures was fitted using equations (3) and (4). All parameter values obtained from the fitting process were then substituted in equations (5), (6), and (7) to estimate the *D*, μ and *n* of the charge carrier in the electrolyte. Figures **10**, **11**, and **12** depicted the charge carrier concentration, mobility, and diffusivity as a function of GG natural polymer concentration at various temperatures.

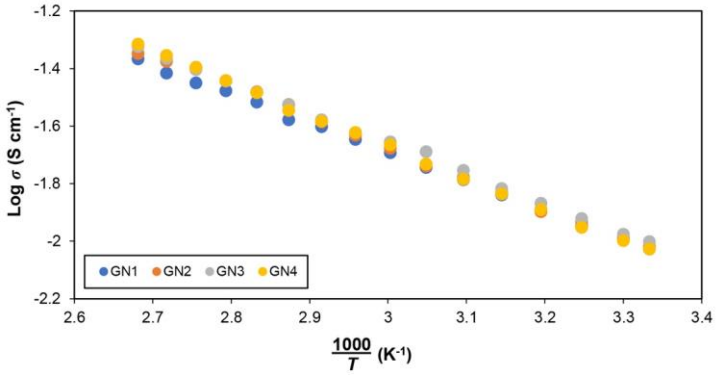

Figure 9: Conductivity-temperature dependence of GG-$LiCF_3SO_3$-DMSO GPE system.

3.5. Evaluation of Ionic Transport Properties at Various Temperature

Figures **10**, **11**, and **12** show the plot of *n*, *μ*, and *D* of charge carriers for the GG-$LiCF_3SO_3$-DMSO GPE system at a temperature range between 300 K and 373 K. Based on Figure **11**, it can be seen that *n* increases along with the increasing temperature. As the temperature increases, the associated ions absorb energy from the heat. This causes each corresponding cation and anion in the $LiCF_3SO_3$ salt to vibrate actively. The binding energy between Li^+ and $CF_3SO_3^-$ becomes weak, and the cation and anion have enough force to break the lattice energy that holds them together and become free ions. As seen in Figure **10**, the plot of *n* mostly overlaps at certain temperatures. This is because the values of *n* are close to each other in all samples. Based on this observation, the number density of charge carriers in GG-$LiCF_3SO_3$-DMSO GPEs increases along with the increasing temperature.

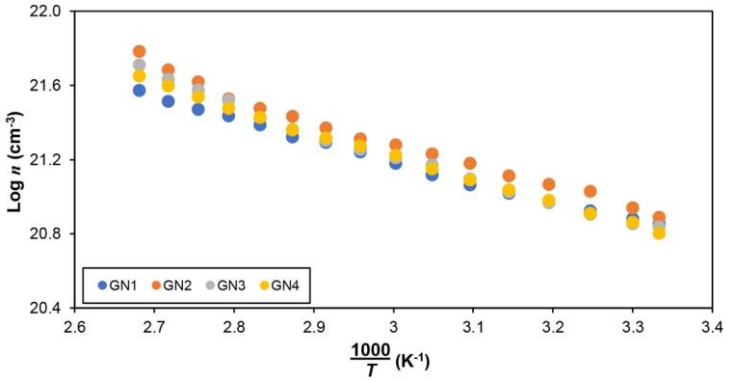

Figure 10: The number density of charge carrier, *n* for GG-$LiCF_3SO_3$-DMSO GPE at various temperatures.

Figures **11** and **12**, respectively show the variation of charge carrier mobility and diffusivity as a function of temperature. It can be seen that *μ* and *D* decrease as the temperature increases in all samples. This phenomenon can be attributed to the increased collision of free ions in the electrolyte. As observed in Figure **10**, *n* increases as the temperature increases. The distance between ions now decreases as the temperature increases. The ions and the GG polymer matrix become close to each other. When an electric field is applied across the sample, the ions move randomly in the confined space, and ion collisions increase. This condition has slowed down the movement of ions, reducing the mobility and diffusivity of charge carriers [38].

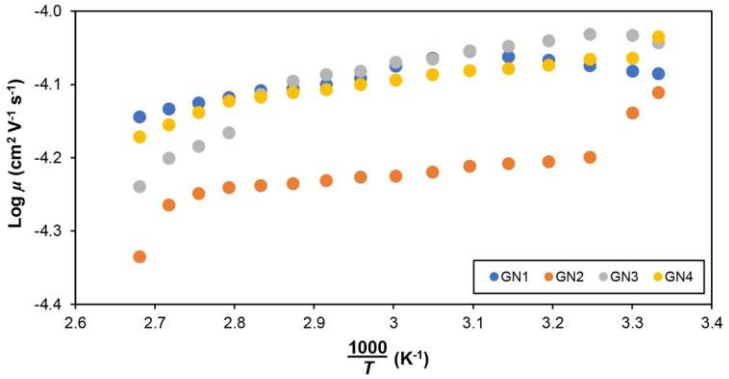

Figure 11: The mobility of charge carrier, *μ* for GG-$LiCF_3SO_3$-DMSO GPE at various temperatures.

3.6. Linear Sweep Voltammetry (LSV)

The high electrochemical stability of electrolytes is an important characteristic before being used in LIBs. Therefore, LSV was performed to study the electrochemical stability window of GPE. Figure **13** shows LSV for 2.00 wt.% GG-12.18 wt.% $LiCF_3SO_3$-85.28 wt.% DMSO GPE (GN3 electrolyte). GN3 electrolyte was selected because it revealed the highest room temperature conductivity value compared to other samples. High conductivity electrolyte is essential to be used as a medium for charge transfer in LIBs.

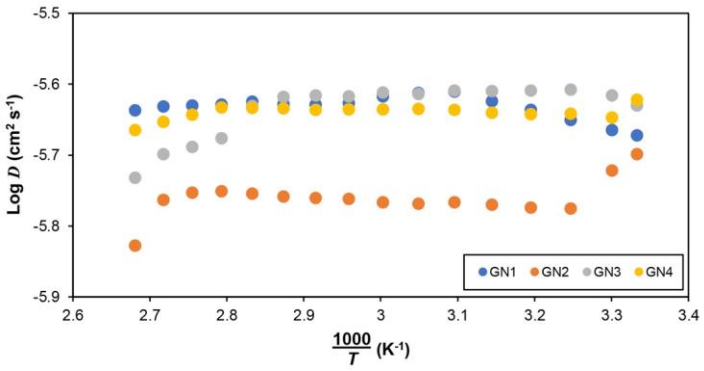

Figure 12: The diffusion coefficient of charge carrier, *D* for GG-LiCF$_3$SO$_3$-DMSO GPE at various temperatures.

LSV measurements have been carried out in a potential window of 0 V to 8.0 V (versus Li/Li$^+$) at a scan rate of 10 mV s^{-1}. As observed in Figure **13**, the current increases suddenly at a voltage of around 4.0 V, indicating an anodic breakdown of the electrolyte due to electrolyte decomposition. The GN3 electrolyte is observed to be stable up to 4.8 V versus Li/Li$^+$. This high cut-off voltage of 4.8 V indicates that the GN3 electrolyte has a good potential to be used as a charge transfer medium in LIBs since the maximum voltage that the cathode materials can withhold in LIBs is less than 4.7 V.

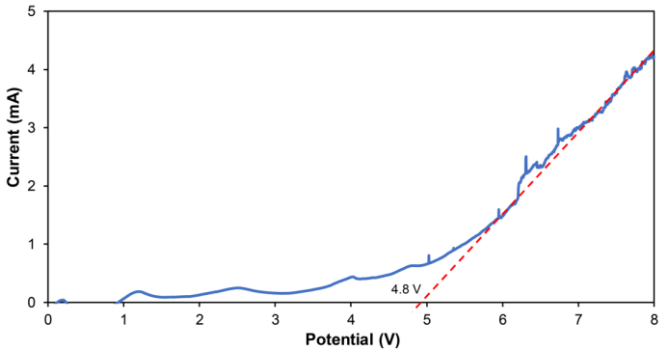

Figure 13: Linear sweep voltammetry of GN3 electrolyte.

3.7. Cyclic Voltammetry (CV)

Figure **14** shows the cyclic voltammogram of the GN3 electrolyte. CV is performed in a potential window between −1.0 V and 5.0 V at a scan rate of 10 mV s^{-1}. The CV process was run through 9 cycles. It can be seen that the cycle areas are identical to each other. This implies that the redox reaction in the GN3 electrolyte is reversible. Good repeatability of the curve for the electrolyte will provide a good LIB cyclic performance [39]. Based on this observation, it can be concluded that the GN3 electrolyte can perform redox processes repeatedly and can be a good candidate for use in rechargeable LIBs as a charge transport medium.

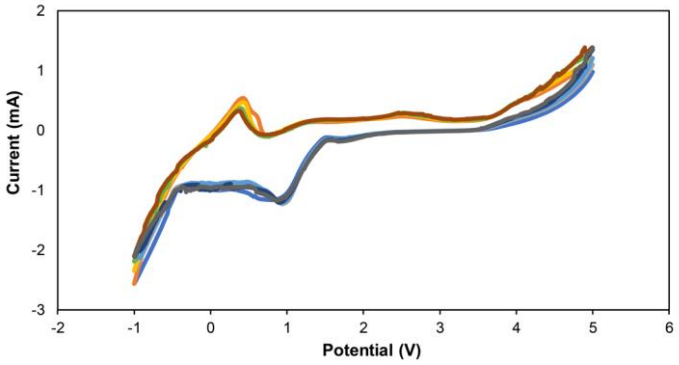

Figure 14: Cyclic voltammogram of GN3 electrolyte.

3.8. Battery-Discharge Performance

Figure **15** shows the discharging curve for LIB with GN3 electrolyte. The LIB is discharged at room temperature with a constant current of 0.001 mA. The low discharge current applied to the battery is because we want to test the potential of the highest conducting GPE prepared in this work in a LIB application. From Figure **15**, it can be seen that the open circuit voltage is 2.86 V. The voltage is observed to drop drastically to 1.98 V after the discharge process for 2.8 hours. A drastic voltage drop may be attributed to the initial discharge process of the battery. The voltage is observed to remain constant with a slight drop of 0.20 V for the next 75.2 hours and drastically decreased to 1.59 V for the next 17 hours. The prepared LIB is observed to retain its voltage at an average of 1.50 V for the next 385 hours (16 days). Based on the result shown in Figure **15**, it can be concluded that the GN3 electrolyte has great potential to be used as an ion transport medium in LIB applications.

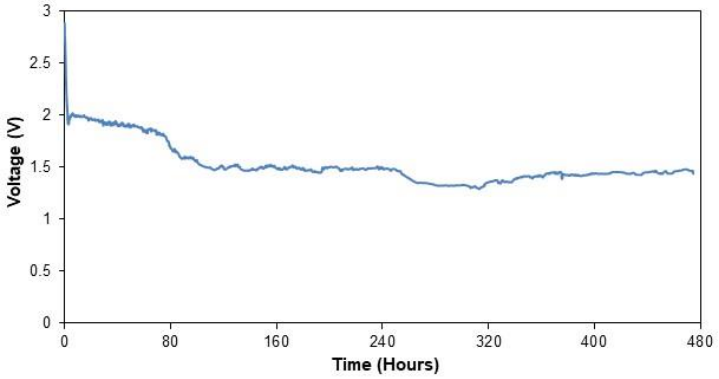

Figure 15: Discharging curve of lithium-ion battery.

4. Conclusion

In this work, two electrolyte systems were successfully prepared, which are $LiCF_3SO_3$-DMSO liquid electrolyte and GG-$LiCF_3SO_3$-DMSO gel polymer electrolyte. For the $LiCF_3SO_3$-DMSO liquid electrolyte system, the room temperature ionic conductivity of DMSO with 0.6 M $LiCF_3SO_3$ of 5.41 mS cm^{-1} increased to a maximum of 9.14 mS cm^{-1} when the $LiCF_3SO_3$ in DMSO increases to 1.0 M (LI3 electrolyte). The conductivity decreased when the amount of $LiCF_3SO_3$ in DMSO exceeded 1.0 M. The conductivity trend in the $LiCF_3SO_3$-DMSO liquid electrolyte system was predominantly controlled by the number density of the charge carrier relative to its mobility. The composition of LI3 electrolyte becomes a reference, whereas the gellan gum (GG) natural polymer was added into the electrolyte to produce gel polymer electrolytes (GPEs). Different GG concentrations were observed to affect the conductivity of the GPE system. The conductivity trend as a function of GG concentration shows the GN3 electrolyte consisting of 2.00 wt.% GG, 12.18 wt.% $LiCF_3SO_3$ and 85.82 wt.% DMSO has the highest room temperature conductivity of 9.96 mS cm^{-1}. The results show that the GG-$LiCF_3SO_3$-DMSO GPE system exhibits a high room temperature conductivity of 10^{-3} S cm^{-1}, proving that GG is one of the promising natural polymers that can be used in lithium-ion batteries (LIBs). Analysis of charge transport properties in GG-$LiCF_3SO_3$-DMSO GPEs shows that the number density of charge carrier (n) was the highest in GN2 electrolyte consisting of 1.72 wt.% GG, 12.21 wt.% $LiCF_3SO_3$ and 86.07 wt.% DMSO.

The trend of mobility (μ) and diffusivity (D) of the charge carriers was observed in the trend opposite to n. The ratio of n to μ indicates that the increase dominantly influenced the increase in conductivity from LI3 electrolyte to GN2 electrolyte in n relative to μ. The rise of conductivity in GN3 electrolyte was strongly controlled by the increase in μ relative to n. The decrease in conductivity in GN4 electrolyte was mainly influenced by the decreased in n, not μ. At various temperatures, the conductivity of GG-$LiCF_3SO_3$-DMSO GPEs increased as the temperature increased from 300 K to 373 K. The increase in conductivity with temperature was dominantly influenced by the increase in the n, not μ. The GN3 electrolyte was used to analyze its electrochemical stability window. The GN3 electrolyte was observed to be electrochemically stable up to 4.8 V. The high electrochemical window indicates that this GN3 electrolyte has good electrochemical stability for use as a charge transfer medium in LIBs. Besides, cyclic

voltammetry (CV) was conducted. The CV process showed an identical cycle area which implies that the redox reaction in GN3 electrolyte is reversible, thus strengthening that this electrolyte is a good candidate as a charge transport medium in rechargeable LIBs. The GN3 electrolyte was used as a charge transport medium in LIBs. The prepared LIB showed a good discharge performance up to 480 hours with an average voltage of 1.50 V with a discharge current of 0.001 mA. Based on the result of discharge-battery performance, it can be concluded that GG-based gel polymer electrolytes have great potential as a charge transport medium in LIB application.

Acknowledgement

I.M. Noor wishes to acknowledge with gratitude the generous funds from the Ministry of Higher Education of Malaysia through the FRGS grant FRGS/1/2020/STG05/UPM/02/1.

References

[1] Bullard N. This Is the Dawning of the Age of the Battery. Bloomberg Green. 2020; 17: 12.

[2] Liu K, Liu Y, Lin D, Pei A, Cui Y. Materials for lithium-ion battery safety. Sci Adv. 2018; 4(6): eaas9820. https://doi.org/10.1126/sciadv.aas9820

[3] Manthiram A. An outlook on lithium ion battery technology. ACS Cent Sci. 2017; 3(10): 1063-9. https://doi.org/10.1021/acscentsci.7b00288

[4] Francis CFJ, Kyratzis IL, Best AS. Lithium-ion battery separators for ionic-liquid electrolytes: a review. Adv Mater. 2020; 32(18): 1904205. https://doi.org/10.1002/adma.201904205

[5] Kim JG, Son B, Mukherjee S, Schuppert N, Bates A, Kwon O, *et al*. A review of lithium and non-lithium based solid state batteries. J Power Sources. 2015; 282: 299-322. https://doi.org/10.1016/j.jpowsour.2015.02.054

[6] Arya A, Sharma AL. Polymer electrolytes for lithium ion batteries: a critical study. Ionics. 2017; 23(3): 497-540. https://doi.org/10.1007/s11581-016-1908-6

[7] Dong D, Zhou B, Sun Y, Zhang H, Zhong G, Dong Q, *et al*. Polymer electrolyte glue: A universal interfacial modification strategy for all-solid-state Li batteries. Nano Lett. 2019; 19(4): 2343-9. https://doi.org/10.1021/acs.nanolett.8b05019

[8] Zhou Q, Ma J, Dong S, Li X, Cui G. Intermolecular chemistry in solid polymer electrolytes for high-energy-density lithium batteries. Adv Mater. 2019; 31(50): 1902029. https://doi.org/10.1002/adma.201902029

[9] Lin Z, Guo X, Wang Z, Wang B, He S, O'Dell LA, *et al*. A wide-temperature superior ionic conductive polymer electrolyte for lithium metal battery. Nano Energy. 2020; 73: 104786. https://doi.org/10.1016/j.nanoen.2020.104786

[10] Jiang Y, Yan X, Ma Z, Mei P, Xiao W, You Q, *et al*. Development of the PEO based solid polymer electrolytes for all-solid state lithium ion batteries. Polymers. 2018; 10(11): 1237. https://doi.org/10.3390/polym10111237

[11] Li W, Pang Y, Liu J, Liu G, Wang Y, Xia Y. A PEO-based gel polymer electrolyte for lithium ion batteries. RSC Adv. 2017; 7(38): 23494-501. https://doi.org/10.1039/C7RA02603J

[12] Nofal MM, Aziz SB, Ghareeb HO, Hadi JM, Dannoun EMA, Al-Saeedi SI. Impedance and dielectric properties of PVC: NH4I solid polymer electrolytes (SPEs): Steps toward the fabrication of SPEs with high resistivity. Materials 2022; 15(6): 2143. https://doi.org/10.3390/ma15062143

[13] Kurapati S, Gunturi SS, Nadella KJ, Erothu H. Novel solid polymer electrolyte based on PMMA: CH_3COOLi effect of salt concentration on optical and conductivity studies. Polym Bull. 2019; 76(10): 5463-81. https://doi.org/10.1007/s00289-018-2659-5

[14] Zhang B, Zhang Y, Zhang N, Liu J, Cong L, Liu J, *et al*. Synthesis and interface stability of polystyrene-poly (ethylene glycol)-polystyrene triblock copolymer as solid-state electrolyte for lithium-metal batteries. J Power Sources. 2019; 428: 93-104. https://doi.org/10.1016/j.jpowsour.2019.04.033

[15] Rani ASM, Rudhziah S, Ahmad A, Mohamed NS. Biopolymer Electrolyte based on derivatives of cellulose from kenaf bast fiber. Polymers. 2014; 6: 2371-85. https://doi.org/10.3390/polym6092371

[16] Rayung M, Min AM, Christirani AS, Chuah AL, Sukor SM, Ahmad A, *et al*. Bio-based polymer electrolytes for electrochemical devices: insight into the ionic conductivity performance. Materials 2020; 13(4): 838. https://doi.org/10.3390/ma13040838

[17] Hamsan MH, Aziz SB, Nofal MM, Brza MA, Abdulwahid RT, Hadi JM, *et al*. Characteristics of EDLC device fabricated from plasticized chitosan: $MgCl_2$ based polymer electrolyte. J Mater Res Technol. 2020; 9(5): 10635-46. https://doi.org/10.1016/j.jmrt.2020.07.096

[18] Abisharani JM, Balamurugan S, Thomas A, Devikala S, Arthanareeswari M, Ganesan S, *et al*. Incorporation of organic additives with electron rich donors (N, O, S) in gelatin gel polymer electrolyte for dye sensitized solar cells. Sol Energy. 2021; 218: 552-62. https://doi.org/10.1016/j.solener.2021.03.007

[19] Colò F, Bella F, Nair JR, Destro M, Gerbaldi C. Cellulose-based novel hybrid polymer electrolytes for green and efficient Na-ion batteries. Electrochim Acta. 2015; 174: 185-90. https://doi.org/10.1016/j.electacta.2015.05.178

[20] Lin Y, Li J, Liu K, Liu Y, Liu J, Wang X. Unique starch polymer electrolyte for high capacity all-solid-state lithium sulfur battery. Green Chem. 2016; 18(13): 3796-803. https://doi.org/10.1039/C6GC00444J

[21] Muthukrishnan M, Shanthi C, Selvasekarapandian S, Manjuladevi R, Perumal P, Selvin CP. Synthesis and characterization of pectin-based biopolymer electrolyte for electrochemical applications. Ionics 2019; 25(1): 203-14. https://doi.org/10.1007/s11581-018-2568-5

[22] Shaari N, Kamarudin SK, Basri S, Shyuan LK, Masdar MS, Nordin D. Enhanced mechanical flexibility and performance of sodium alginate polymer electrolyte bio-membrane for application in direct methanol fuel cell. J Appl Polym Sci. 2018; 135(37): 46666. https://doi.org/10.1002/app.46666

[23] Priya SS, Karthika M, Selvasekarapandian S, Manjuladevi R. Preparation and characterization of polymer electrolyte based on biopolymer I-Carrageenan with magnesium nitrate. Solid State Ion. 2018; 327: 136-49. https://doi.org/10.1016/j.ssi.2018.10.031

[24] Noor IM. Determination of charge carrier transport properties of gellan gum-lithium triflate solid polymer electrolyte from vibrational spectroscopy. High Perform Polym. 2020; 32(2): 168-74. https://doi.org/10.1177/0954008319890016

[25] Noor ISM, Majid SR, Arof AK, Djurado D, Claro Neto S, Pawlicka A. Characteristics of gellan gum-LiCF$_3$SO$_3$ polymer electrolytes. Solid State Ion. 2012; 225: 649-53. https://doi.org/10.1016/j.ssi.2012.03.019

[26] Iwata T. Biodegradable and bio-based polymers: future prospects of eco-friendly plastics. Angew Chem Int Ed Engl. 2015; 54(11): 3210-5. https://doi.org/10.1002/anie.201410770

[27] Dave PN, Gor A. Natural polysaccharide-based hydrogels and nanomaterials: Recent trends and their applications. In: Hussain CM, Eds. Handbook of nanomaterials for industrial applications. 1st ed. Elsevier: 2018; pp. 36-66. https://doi.org/10.1016/B978-0-12-813351-4.00003-1

[28] Gupta S, Variyar PS. Guar gum: a versatile polymer for the food industry. In: Grumezescu AM, Holban AM, Eds. Biopolymers for food design. Academic Press: 2018; pp. 383-407. https://doi.org/10.1016/B978-0-12-811449-0.00012-8

[29] Halim NFA, Majid SR, Arof AK, Kajzar F, Pawlicka A. Gellan Gum-LiI gel polymer electrolytes. Mol Cryst Liq Cryst. 2012; 554(1): 232-8. https://doi.org/10.1080/15421406.2012.634344

[30] Neto MJ, Sentanin F, Esperança JMSS, Medeiros MJ, Pawlicka A, de Zea Bermudez V, *et al*. Gellan gum - Ionic liquid membranes for electrochromic device application. Solid State Ion. 2015; 274: 64-70. https://doi.org/10.1016/j.ssi.2015.02.011

[31] Ren W, Ding C, Fu X, Huang Y. Advanced gel polymer electrolytes for safe and durable lithium metal batteries: Challenges, strategies, and perspectives. Energy Stor Mater. 2021; 34: 515-35. https://doi.org/10.1016/j.ensm.2020.10.018

[32] Arof AK, Amirudin S, Yusof SZ, Noor IM. A method based on impedance spectroscopy to determine transport properties of polymer electrolytes. Phys Chem Chem Phys. 2014; 16(5): 1856-67. https://doi.org/10.1039/C3CP53830C

[33] Careem MA, Noor ISM, Arof AK. impedance spectroscopy in polymer electrolyte characterization. In: Winie T, Arof AK, Thomas S, Eds. Polymer Electrolytes. Wiley; 2020; pp. 23-64. https://doi.org/10.1002/9783527805457.ch2

[34] Arof AK, Noor IM, Buraidah MH, Bandara TMWJ, Careem MA, Albinsson I, *et al*. Polyacrylonitrile gel polymer electrolyte based dye sensitized solar cells for a prototype solar panel. Electrochim Acta. 2017; 251: 223-34. https://doi.org/10.1016/j.electacta.2017.08.129

[35] Noor ISM. Characterization and transport properties of PVA-LiBOB based polymer electrolytes with application in dye sensitized solar cells. University of Malaya, Malaysia; 2016.

[36] Ghanadzadeh Gilani A, Moghadam M, Ghorbanpour T. Dielectric study of H-bonded interactions in amyl alcohols with ketones and DMSO at T = 298.15 K. J Chem Thermodyn. 2017; 113: 263-75. https://doi.org/10.1016/j.jct.2017.06.020

[37] Noor IS, Majid SR, Arof AK. Poly(vinyl alcohol)-LiBOB complexes for lithium-air cells. Electrochim Acta. 2013; 102: 149-60. https://doi.org/10.1016/j.electacta.2013.04.010

[38] Chowdhury FI, Buraidah MH, Arof AK, Mellander BE, Noor IM. Impact of tetrabutylammonium, iodide and triiodide ions conductivity in polyacrylonitrile based electrolyte on DSSC performance. Sol Energy. 2020; 196: 379-88. https://doi.org/10.1016/j.solener.2019.12.033

[39] Abidin SZZ, Ali AMM, Hassan OH, Yahya MZA, Electrochemical studies on cellulose acetate-LiBOB polymer gel electrolytes. Int J Electrochem Sci. 2013; 8: 7320-6.